2013 European Control Conference (ECC)
July 17-19, 2013, Zürich, Switzerland.

Nonlinear Stability Analysis of DFIG Wind Generators in Voltage Oriented Control Operation

Michael K. Bourdoulis, *Student Member, IEEE*, and Antonio T. Alexandridis, *Member, IEEE*

***Abstract*—In this paper the damping and stability properties of Doubly-Fed Induction Generator (DFIG) wind systems are studied. First the complete 5th order nonlinear system of a DFIG in the synchronously rotating *dq* reference frame is introduced. Assuming operation under the grid voltage oriented control mode, it is possible to control reactive and active power separately through the *d* and *q* controlled voltage inputs, respectively. After that, a simple cascaded controller design is adopted for each input, comprising of proportional inner-loop and proportional-integral outer-loop controllers. A passivity analysis is conducted for both the open- and closed-loop systems with the dynamics of the proportional inner-loop controllers taken into account. The analysis shows that the damping of the system can be modulated by the inner-loop controllers while it provides an appropriate storage function for the nonlinear stability analysis. This constitutes the main contribution of the paper since it is the first time that stability and convergence to the equilibrium is proven for the complete machine model in the face of unknown torque inputs, without needing any estimation or adaptive mechanism. Finally, the analysis and the performance of the closed-loop DFIG wind system are verified through extensive simulation results.**

***Index Terms*—Nonlinear stability, passivity, variable-speed wind systems, induction machine.**

I. Introduction

The Doubly-fed induction generator (DFIG) based wind system is a widely used option of the variable speed concept, for up to 3MW individual generator ratings [1]. It provides a possibility of variable speed regulation of about ±30% around the synchronous speed. A wound rotor induction machine (generator) is utilized with its stator directly connected to the grid, while the rotor is connected to the grid through a frequency converter comprising of two back-to-back ac/dc converters with a dc-link [2], as shown in Fig. 1.

Variable speed regulation is essential for the optimal operation of a wind generator system. It achieves a continuous tracking of the rotating speed in a manner that: a) it adapts the turbine speed at a reference level as it is determined by the measured average wind speed value which corresponds to the maximum power extraction [3], b) it provides an improved power quality and network stability [4]. Therefore, an effective, stable and fast control design acting on the induction generator rotor side is needed to fulfill this requirement. However, since the induction machine is a nonlinear system, this control design is not an easy task.

Vector or Field Oriented Control (FOC) is the standard mode used for the control design of induction machines [5]. In this mode the system frame is aligned with the rotor or the stator flux (field orientation). Especially for DFIGs, the standard method used [5]-[7] is the stator-FOC one. This prerequires the system model to be represented in the synchronously rotating *dq* reference frame. The benefits of this *dq* reference model are that both the coupling stator and rotor coils as well as the steady state variables and inputs (currents, fluxes, speed and voltages) become constant. As a result, two controlled inputs are appeared corresponding to the *d* and *q* components of the rotor voltage on which usually PI controllers are implemented. The structure of two cascaded controllers is used at each input, with the inner-loops regulating the *d* and *q* current components while exact cancelation networks for decoupled operation are utilized [3], [7]-[8]. The outer-loop PI controllers provide the reference current values and they are tuned to have a slower response than those of the inner-loop, a feature typical for cascaded controllers, known as time-scale separation assumption.

Particularly, an outer-loop PI controller which regulates the generator's rotational speed to the optimum corresponding to the maximum wind power extraction provides a reference current for the first inner-loop current controller. The other reference current is usually provided by an outer-loop PI controller that regulates the stator's reactive power [6]-[7].

However, as it was proven in [9], the linearized DFIG system has two poorly damped poles with their oscillating frequency close to the power grid frequency. As a result, in order for the system to be stable when stator-FOC is adopted, a constraint for the *d*-axis component of the rotor current's maximum value has to be set. On the other hand, it has been proven that an alternative orientation can be used, namely the grid-Voltage Oriented Control (VOC). When VOC is adopted, obviously the system frame is aligned on the grid voltage, with main advantages the improved damping of these poles and an easy implementation.

In this paper, after obtaining in state-space the complete 5th order nonlinear DFIG system model, we adopt the VOC approach to propose a simplified cascaded control scheme at the rotor side *dq* voltage inputs. The cascaded controllers

M. K. Bourdoulis is with the Electrical and Computer Engineering Department, University of Patras, Patras, 26500 Greece (phone: +30-2610-997699; fax: +30-2610-996803; e-mail: bourdoulis@ece.upatras.gr).

A. T. Alexandridis is with the Electrical and Computer Engineering Department, University of Patras, Patras, 26500 Greece (e-mail: a.t.alexandridis@ece.upatras.gr).

consist of proportional inner-loop controllers, with no decoupling networks utilized, and standard PI outer-loop controllers. Then for the open-loop system, we discuss its damping properties by proving system passivity. Furthermore, taking into account inner-loop controllers, we prove that the system renders the passivity property by partially shaping its damping characteristics. Since passivity provides an easy way for obtaining Lyapunov-type storage functions, it gives a useful tool of studying system stability. In particular, since the system is fully damped, it is proven that global exponential stability of the closed-loop unforced system holds true and consequently that the input-to-state stability (ISS) of the original closed-loop system is ensured. As it has been recently proven in [10], ISS property of passive systems is essential for also proving convergence to the equilibrium. Thus, in the paper, we show that the DFIG system belongs to this category of passive systems and therefore it satisfies stability and convergence to the equilibrium. At this point we note that whenever global asymptotic stability has been proven, this is certainly based on the reduced-order current fed model of the machine, i.e. on the 3rd order system with states the rotor fluxes and the rotating speed and controlled inputs the stator currents [11]-[12]. In some research works where the 5th order model is used, asymptotic stability is proven only under the use of load torque estimators or adaptation techniques [13]-[15]. The simulation results confirm the theoretical analysis indicating the effectiveness of the proposed cascaded control design approach.

II. Modeling and Analysis of the Doubly-Fed Induction Generator

A. System Modeling in the dq Reference Frame

The dynamic model of a DFIG with states and inputs in the *dq* synchronously rotating frame can be written as [16]

$$\begin{aligned} U_{ds} &= \dot{\lambda}_{ds} - \omega_s \lambda_{qs} + R_s I_{ds} \\ U_{qs} &= \dot{\lambda}_{qs} + \omega_s \lambda_{ds} + R_s I_{qs} \\ V_{dr} &= \dot{\lambda}_{dr} - (\omega_s - p\omega_r)\lambda_{qr} + R_r I_{dr} \\ V_{qr} &= \dot{\lambda}_{qr} + (\omega_s - p\omega_r)\lambda_{dr} + R_r I_{qr} \end{aligned} \tag{1}$$

with

$$\begin{aligned} \lambda_{ds} &= L_s I_{ds} + L_m I_{dr} \quad \lambda_{dr} = L_r I_{dr} + L_m I_{ds} \\ \lambda_{qs} &= L_s I_{qs} + L_m I_{qr} \quad \lambda_{qr} = L_r I_{qr} + L_m I_{qs} \end{aligned} \tag{2}$$

$$J\dot{\omega}_r + b\omega_r = \frac{3}{2} p \frac{L_m}{L_s}(\lambda_{qs} I_{dr} - \lambda_{ds} I_{qr}) - T_m \tag{3}$$

Equations (1) and (3) represent the complete electromechanical dynamics of the DFIG system, while the active and reactive power expressions for the stator and rotor are as follows

$$\begin{aligned} P_s &= \frac{3}{2}(U_{ds} I_{ds} + U_{qs} I_{qs}) \quad Q_s = \frac{3}{2}(U_{qs} I_{ds} - U_{ds} I_{qs}) \\ P_r &= \frac{3}{2}(V_{dr} I_{dr} + V_{qr} I_{qr}) \quad Q_r = \frac{3}{2}(V_{qr} I_{dr} - V_{dr} I_{qr}) \end{aligned} \tag{4}$$

where *d* and *q* subscripts stand for the *d*- and *q*-axis components, *r* and *s* subscripts stand for rotor and stator, U stands for the constant grid voltage and V for variable voltage, λ stands for flux, R stands for resistance, I stands for current, ω_s stands for the utility frequency, p stands for the number of pole pairs, ω_r stands for the rotational speed of the generator rotor, L stands for inductance and L_m is the mutual inductance, J is the total moment of inertia at the rotor of the induction generator, *b* is the damping coefficient, T_m is the mechanical torque at the rotor, while P and Q stand for active and reactive power. The dot over a symbol stands for the time derivative of the corresponding variable.

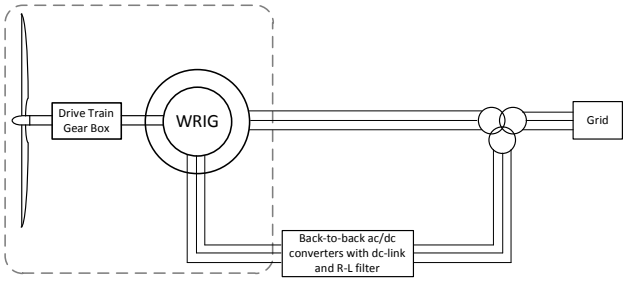

Fig. 1. The DFIG wind system.

B. State-Space Modeling of the DFIG

Using (1)-(3) and selecting $x = [I_{ds}\ I_{qs}\ I_{dr}\ I_{qr}\ \omega_r]^T$ as the state vector, the complete 5th order dynamic model is obtained, where $\sigma = (L_r L_s - L_m^2)/(L_r L_s)$ denotes the leakage factor.

In this model, show in the next, V_{dr} and V_{qr} are the control inputs fed by the voltage source converter at the rotor side, while U_{ds}, U_{qs} are the uncontrolled inputs representing the *d* and *q* components of the grid voltage and T_m is considered to be the unknown load disturbance input.

$$
\begin{bmatrix}
\sigma L_s & & & & \\
 & \sigma L_s & & 0 & \\
 & & \sigma L_r & & \\
 & 0 & & \sigma L_r & \\
 & & & & J
\end{bmatrix}
\frac{d}{dt}
\begin{bmatrix} I_{ds} \\ I_{qs} \\ I_{dr} \\ I_{qr} \\ \omega_r \end{bmatrix} =
$$

$$
\begin{bmatrix}
-R_s & \omega_s \sigma L_s & R_r \frac{L_m}{L_r} & p\omega_r L_m & p\frac{L_m^2}{L_r} I_{qs} \\
-\omega_s \sigma L_s & -R_s & -p\omega_r L_m & R_r \frac{L_m}{L_r} & -p\frac{L_m^2}{L_r} I_{qs} \\
R_s & -p\omega_r L_s & -R_r \frac{L_m}{L_r} & \omega_s \sigma L_r & -p\frac{L_r L_s}{L_m} I_{qr} \\
p\omega_r L_s & R_s & -\omega_s \sigma L_r & -R_r \frac{L_m}{L_r} & p\frac{L_r L_s}{L_m} I_{dr} \\
-\frac{3}{2} p L_m I_{qr} & \frac{3}{2} p L_m I_{dr} & 0 & 0 & -b
\end{bmatrix}
\begin{bmatrix} I_{ds} \\ I_{qs} \\ I_{dr} \\ I_{qr} \\ \omega_r \end{bmatrix} +
$$

$$
+ \begin{bmatrix}
-\frac{L_m}{L_r} & 0 \\
0 & -\frac{L_m}{L_r} \\
\frac{L_s}{L_m} & 0 \\
0 & \frac{L_s}{L_m} \\
0 & 0
\end{bmatrix}
\begin{bmatrix} V_{dr} \\ V_{qr} \end{bmatrix} +
\begin{bmatrix}
1 & 0 & 0 \\
0 & 1 & 0 \\
-1 & 0 & 0 \\
0 & -1 & 0 \\
0 & 0 & -1
\end{bmatrix}
\begin{bmatrix} U_{ds} \\ U_{qs} \\ T_m \end{bmatrix} \tag{5}
$$

III. Induction Machine Controller Tasks

A. Voltage-Oriented Control Preliminaries

In the case studied, where the VOC technique is applied, the reference frame is chosen to align with the q-axis component of the stator voltage, which means that U_{ds}=0. Using the first two differential equations of (1) at steady state and for the adopted VOC, the following hold true:

$$
\begin{aligned}
0 &= -\omega_s \lambda_{qs} + R_s I_{ds} \\
U_{qs} &= \omega_s \lambda_{ds} + R_s I_{qs}
\end{aligned} \tag{6}
$$

or equivalently

$$
\begin{aligned}
\lambda_{qs} &= \frac{R_s}{\omega_s} I_{ds} \\
\lambda_{ds} &= \frac{R_s I_{qs} - U_{qs}}{\omega_s}
\end{aligned} \tag{7}
$$

For induction generators of MW ratings, the stator resistance is valued at the range of $m\Omega$ and $\omega_s = 100\pi \; rad/\sec$. As a result, the q-axis stator flux component has a very small value at steady state, while for the d-axis stator flux component it holds that

$$
\lambda_{ds} \cong -\frac{U_{qs}}{\omega_s} \tag{8}
$$

This approximation reduces the electromagnetic torque expression (3) to

$$
T_e = -\frac{3}{2} p \frac{L_m}{L_s} \lambda_{ds} I_{qr} \tag{9}
$$

It is obvious that for an almost constant value of λ_{ds}, as given by (8), the electromagnetic torque depends only on the q-axis component I_{qr} of the rotor current.

B. Active and Reactive Power Regulation

The mechanical power captured from the wind by the turbine is given by [17]

$$
P_m = \frac{1}{2} \rho \pi R^2 C_p(\lambda, \beta) v_{wind}^3 \tag{10}
$$

where ρ is the air density, R is the radius of the turbine blades, v_{wind} is the wind speed, C_p is the power coefficient of the wind turbine, β is the blade pitch angle and λ is the tip-speed ratio.

In order to achieve maximum active power extraction, the maximum value of C_p should be achieved for some constant λ=λ_{opt}. This can be achieved through the optimal rotational speed of the generator, provided by [3]

$$
\omega_{r,opt} = \frac{\lambda_{opt} n_g}{R} v_{wind} \tag{11}
$$

where n_g is the gear ratio due to the existence of a gearbox.

Thus, the wind speed v_{wind} determines through (11) the rotor generator speed that corresponds to the maximum wind power extraction. As a result, one of the rotor side controller tasks is to adapt the generator speed ω_r to a reference $\omega_r^{ref} = \omega_{r,opt}$. Taking into account (9), one can see that for any wind speed v_{wind} the inner-loop current I_{qr} controller enforces T_e to follow T_m by regulating I_{qr} to a suitable I_{qr}^{ref}; this reference value obviously comes from an outer-loop PI controller which regulates ω_r to ω_r^{ref} corresponding to the maximum T_m.

In the same way, it can be easily shown that reactive stator power can be regulated through the I_{dr} inner current control loop, since Q_s is dependent from I_{dr}. Indeed, combining the λ_{ds} expression from (2) and the Q_s expression from (4), while the proposed VOC holds true, the following expression is easily reached:

$$
\lambda_{ds} = \frac{2}{3} L_s \frac{Q_s}{U_{qs}} + L_m I_{dr} \tag{12}
$$

It is clear from (12) that the stator reactive power can be regulated through I_{dr}. A common way to determine I_{dr}^{ref} is by enforcing Q_s to a desired reference value through an outer loop PI controller.

Therefore, an effective active and reactive power regulation can be eventually achieved by VOC, provided that system stability and convergence to the equilibrium is guaranteed. In the following section, this stability analysis is obtained via a passivity analysis and controller design.

IV. Control Design and Analysis

A. The Proposed Control Scheme

A cascaded control scheme with proportional inner-loop and conventional PI outer-loop controllers is proposed as follows.

1) *d*-axis cascaded controllers

The following inner-loop current controller is proposed for the rotor input V_{dr}

$$V_{dr} = k_{Pd}\left(I_{dr}^{ref} - I_{dr}\right) \tag{13}$$

where the reference input I_{dr}^{ref} is provided by an outer-loop PI controller, as follows

$$I_{dr}^{ref} = k_{PQ}\left(Q_s^{ref} - Q_s\right) + k_{IQ}\int_0^t \left(Q_s^{ref} - Q_s\right) d\tau \tag{14}$$

The proportional and integral gains k_{Pd}, k_{PQ} and k_{IQ} are positive scalars.

2) *q*-axis cascaded controllers

For V_{qr} the following inner-loop proportional controller is proposed

$$V_{qr} = k_{Pq}\left(I_{qr}^{ref} - I_{qr}\right) \tag{15}$$

where now the reference input I_{qr}^{ref} is provided by an outer-loop PI controller, as follows

$$I_{qr}^{ref} = -k_{P\omega}\omega_r + k_{I\omega}\int_0^t \left(\omega_r^{ref} - \omega_r\right) d\tau \tag{16}$$

All the proportional and integral gains k_{Pq}, $k_{P\omega}$ and $k_{I\omega}$ are positive scalars and ω_r^{ref} is provided by (11).

Both the outer-loop PI controllers should be much slower than the inner-loop controllers.

Now, to proceed with the dynamic and stability analysis of the aforementioned system, we start by investigating its damping characteristics. Therefore, since passivity is strongly related to the system damping, we first analyze the closed-loop passivity property.

B. Closed-loop System Passivity

In order to use Theorem 1 of Appendix, consider for system (5) the following (Lyapunov type) storage function

$$V = \frac{3}{4}L_s(I_{ds}^2 + I_{qs}^2) + \frac{3}{2}L_m(I_{ds}I_{dr} + I_{qs}I_{qr}) + \\ + \frac{3}{4}L_r(I_{dr}^2 + I_{qr}^2) + \frac{1}{2}J\omega_r^2 \tag{17}$$

which is positive definite since $L_s, L_r > L_m$ holds true and and

$$V > \frac{3}{4}L_m(I_{ds} + I_{dr})^2 + \frac{3}{4}L_m(I_{qs} + I_{qr})^2 + \frac{1}{2}J\omega_r^2$$

Taking into account in (5) the proportional inner-loop controllers (13) and (15), the storage function derivative is calculated as Then the time derivative of V is calculated as

$$\dot{V} = -\frac{3}{2}\left[R_s I_{ds}^2 + R_s I_{qs}^2 + \left(R_r + k_{Pd}\right) I_{dr}^2 + \left(R_r + k_{Pq}\right) I_{qr}^2\right] - \\ - b\omega_r^2 + \frac{3}{2}(I_{ds}U_{ds} + I_{qs}U_{qs} + k_{Pd}I_{dr}I_{dr}^{ref} + k_{Pq}I_{qr}I_{qr}^{ref}) - \\ - \omega_r T_m \tag{18}$$

where the first five terms of V derivative indicate the closed-loop system damping characteristics corresponding to the power dissipated at the electrical and mechanical parts describing a fully damped system and increased by k_{Pd} and k_{Pq} at the rotor-side dynamics. The latter expression implies the following inequality

$$\dot{V} \le \frac{3}{2}(I_{ds}U_{ds} + I_{qs}U_{qs} + k_{Pd}I_{dr}I_{dr}^{ref} + k_{Pq}I_{qr}I_{qr}^{ref}) - \\ - \omega_r T_m = y^T u \tag{19}$$

where $y = G^T x$, $G = diag\{3/2, 3/2, 3k_{Pd}/2, 3k_{Pq}/2, 1\}$, $x = [I_{ds}\ I_{qs}\ I_{dr}\ I_{qr}\ \omega_r]^T$ and $u = [U_{ds}\ U_{qs}\ I_{dr}^{ref}\ I_{qr}^{ref}\ -T_m]^T$.

Inequality (19) clearly indicates that the closed-loop system is passive for output $y = G^T x$ [18].

It is noted that the passivity property also holds true for the open-loop system with storage function the same used for the closed-loop system.

C. Closed-loop System Stability Analysis

At this point, we are ready to exploit the closed-loop passivity property on proving stability. Hence, we start by investigating the nonautonomous closed-loop unforced system, i.e. the closed-loop system with $u = 0$. For the unforced system, we obtain from (18) the following negative definite expression of the storage function time derivative

$$\dot{V} = -\frac{3}{2}\left[R_s I_{ds}^2 + R_s I_{qs}^2 + \left(R_r + k_{Pd}\right) I_{dr}^2 + \left(R_r + k_{Pq}\right) I_{qr}^2\right] - b\omega_r^2$$

Now, recalling [18, Theorem 4.10, p. 154] for the dynamic closed-loop system, one can easily observe that all assumptions required hold true, since both V and $-\dot{V}$ are in quadratic form and positive definite. Therefore, the origin $x = 0$ is globally exponentially stable.

Coming back to the original closed-loop system with input $u \neq 0$, [18, Lemma 4.6, pp. 176-177] holds true (since *g(x)* is constant and *f(x)* satisfies the Lipschitz conditions) indicating that the closed-loop system is input-to-state stable (ISS).

Therefore, the original closed-loop system is passive with a bounded solution. As a result, all the pre-required conditions mentioned in [10], namely Assumptions 1, 2 and Theorem 4 of [10], are satisfied. Hence, the closed-loop system is stable and converges to the equilibrium.

This analysis guarantees that the proposed cascaded control scheme can be utilized, while the passivity property is preserved and all conditions to ensure closed-loop stability are satisfied. Also, since the proof is independent from any field or voltage orientation, the adopted VOC in this paper can be effectively applied in steady state.

V. Simulation Results

In this section, the effectiveness of the proposed controller design and analysis is verified through extensive simulation results. The response of the DFIG system is simulated for the case of step changes in the wind speed, as shown in Fig. 2, and the reactive power reference. All the parameters of the simulated system are provided in Table I. The control parameters are selected to be k_{Pd}=1, k_{Pq}=5, $k_{P\omega}$=30, $k_{I\omega}$=10, k_{PQ}=0.0001 and k_{IQ}=0.01.

Figure 2 also presents the generator's rotor angular speed versus its reference, where it clear that ω_r tracks its reference well and has a rather small settling time of about 15sec. In Fig. 3 the responses of the *d*- and *q*-axis components of the stator current are presented. It is clear that I_{ds} response is associated with the reactive power reference, as expected from the expression of Q_s in (4) for the adopted VOC. On the other hand, I_{qs} response follows the form of ω_r and is associated with the active power reference, as expected from the expression of P_s in (4) for the adopted VOC.

Figure 4 provides the responses of the *d*- and *q*-axis rotor current components. As expected, the response of I_{dr} is associated with that of Q_s, while I_{qr} quickly reaches its steady state value and follows the mechanical torque changes caused by the wind step changes.

TABLE I
2MW DFIG WIND SYSTEM PARAMETERS

Symbol	Quantity	Value
R_s	stator resistance	0.01 Ω
R_r	rotor resistance	0.00842 Ω
L_s	stator inductance	0.005305 H
L_r	rotor inductance	0.0053137 H
L_m	mutual inductance	0.0051839 H
p	pole pairs	3
R	blade radius	35 m
b	rotor friction coefficient	0.00015 $N*m*sec/rad$
J	rotor inertia	765.6 $kg*m^2$
n_g	gearbox ratio	62.5
β	pitch angle	0°
ρ	air density	1.2 kg/m^3
λ_{opt}	optimal tip-speed-ratio	6.325
ω_s	grid angular frequency	2π50 rad/sec
$\sqrt{U_{ds}^2+U_{qs}^2}$	grid voltage	700 V (rms)

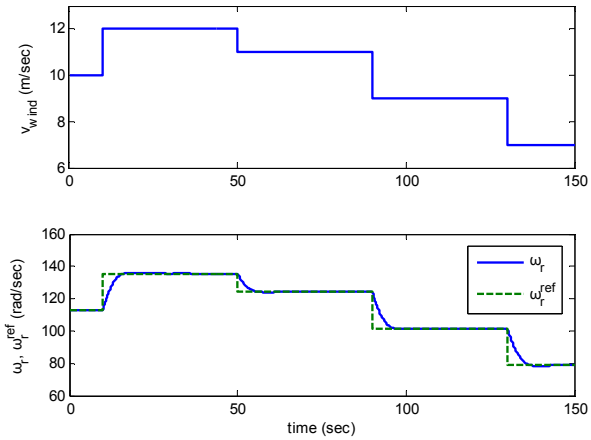

Fig. 2. Wind speed profile and rotor angular speed with its reference.

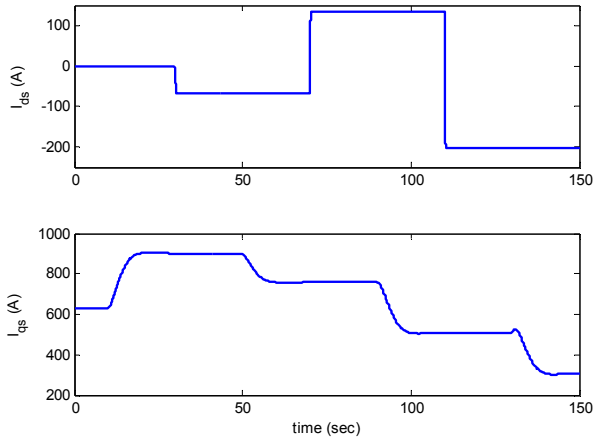

Fig. 3. Stator current component responses.

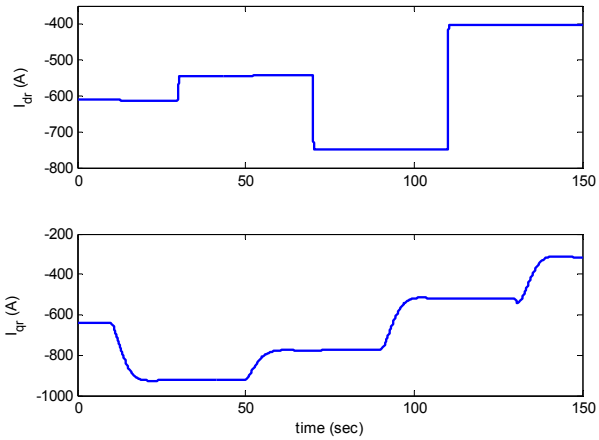

Fig. 4. Rotor current component responses.

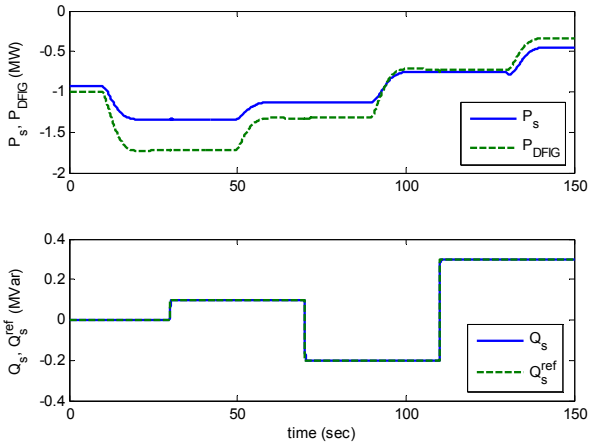

Fig. 5. Active and reactive power responses.

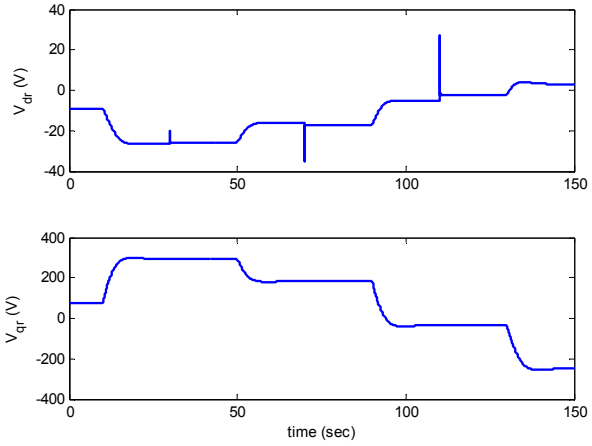

Fig. 6. Rotor voltage control input responses.

Figure 5 represents the stator's and total DFIG active power, while also the response of the stator's reactive power versus its reference is provided. Both active power responses reach their steady state values in less than 20sec, while the reactive power rapidly tracks its reference.

Finally, Fig. 6 provides the responses of V_{dr} and V_{qr}, which are the control inputs. Both voltages exhibit satisfactory transient performance and converge to admissible values.

VI. Conclusion

A simple cascaded control scheme for DFIGs under VOC has been proposed, comprising of proportional inner-loop *d* and *q* current controllers and conventional PI outer-loop speed and reactive power controllers. A novel nonlinear analysis has been conducted to prove stability and convergence to the equilibrium. Finally, the effectiveness of the proposed control scheme is verified through extensive simulation results.

References

[1] R. Teodorescu, M. Liserre, and P. Rodriguez, *Grid Converters for Photovoltaic and Wind Power Systems*. West Sussex, UK: Wiley-IEEE Press, 2011.

[2] R. Pena, J. C. Clare, and G. M. Asher, "Doubly fed induction generator using back-to-back PWM converters and its application to variable speed wind-energy generation," *Proc. IEE- Elect. Power Appl.*, vol. 143, no. 3, pp. 231–241, May 1996.

[3] M. K. Bourdoulis, and A. T. Alexandridis, "PI Control Design and Passivity/Stability Analysis for DFIG Wind Systems under Vector Control Constraints," *in 14th IASTED International Conference on Control and Applications (IASTED CA 2012)*, Crete, Greece, Jun. 18-20, 2012, pp. 127-134.

[4] A. D. Hansen, C. Jauch, P. Sørensen, F. Iov, and F. Blaabjerg, "Dynamic wind turbine models in power system simulation tool DIgSILENT," Risø National Laboratory, Risø, Denmark, Tech. Rep. Risø-R-1400(EN), Dec. 2003.

[5] G. Abad, G. Iwanski, J. López, L. Marroyo, and M. A. Rodríguez, *Doubly Fed Induction Machine: Modeling and Control for Wind Energy Generation Applications*. Hoboken, NJ: Wiley, 2011.

[6] A. D. Hansen, P. Sørensen, F. Iov, and F. Blaabjerg, "Control of variable speed wind turbines with doubly-fed induction generators," Wind Eng., vol. 28, no. 4, pp. 411–434, June 2004.

[7] W. Qiao, W. Zhou, J. M. Aller, and R. G. Harley, "Wind Speed Estimation Based Sensorless Output Maximization Control for a Wind Turbine Driving a DFIG," *IEEE Trans. Power Electron.*, vol. 23, no. 3, pp. 1156–1169, May 2008.

[8] A. Yazdani, and R. Iravani, *Voltage-Sourced Converters: Modeling, Control, and Applications*. Hoboken, NJ: Wiley, 2010.

[9] A. Petersson, L. Harnefors, and T. Thiringer, "Comparison between stator flux and grid flux oriented rotor current control of doubly-fed induction generators," *in Proc. 35th IEEE Power Electr. Spec. Conf.*, Aachen, Germany, 2004, pp. 482–486.

[10] G. C. Konstantopoulos, and A. T. Alexandridis, "Stability and Convergence Analysis for a Class of Nonlinear Passive Systems," *in 50th IEEE Conference on Decision and Control and European Control Conference (IEEE CDC-ECC 2011)*, Orlando, FL, Dec. 12-15, 2011, pp. 1753-1758.

[11] P. A. S. De Wit, R. Ortega, and I. Mareels, "Indirect Field-oriented Control of Induction Motors is Robustly Globally Stable," *Automatica*, vol. 32, no. 10, pp. 1393–1402, 1996.

[12] R. Reginatto, and A. S. Bazanella, "Robustness of Global Asymptotic Stability in Indirect Field-Oriented Control of Induction Motors," *IEEE Trans. Aut. Control*, vol. 48, no. 7, pp. 1218–1222, July 2003.

[13] D. Karagiannis, A. Astolfi, R. Ortega, and Mickaël Hilairet, "A Nonlinear Tracking Controller for Voltage-Fed Induction Motors With Uncertain Load Torque," *IEEE Trans. Control Syst. Tech.*, vol. 17, no. 3, pp. 608–619, May 2009.

[14] V. M. Hernandez-Guzman, and V. Santibanez, "A saturated PI velocity controller for voltage-fed induction motors," *European Journal of Control.*, vol. 18, no. 1, pp. 58–68, 2012.

[15] H. E. Psillakis, A. T. Alexandridis, L. Marconi, and A. Tilli, "Discussion on: "A Saturated PI Velocity Controller for Voltage-Fed Induction Motors," *European Journal of Control.*, vol. 18, no. 1, pp. 69–73, 2012.

[16] P. C. Krause, O. Wasynczuk, and S. D. Sudhoff, *Analysis of Electric Machinery and Drive Systems, 2nd Edition*. Piscataway, NJ: Wiley-IEEE Press, 2002.

[17] L. Yang, Z. Xu, J. Østergaard, Z. Y. Dong, and K. P. Wong, "Advanced Control Strategy of DFIG Wind Turbines for Power System Fault Ride Through," *IEEE Trans. Power Systems*, vol. 27, no. 2, pp. 713–722, May 2012.

[18] H. K. Khalil, *Nonlinear Systems, 3rd Edition*, Upper Saddle River, NJ: Prentice-Hall, 2002.